Supporting Information for

Shape-tunable Pt-Ir Alloy Nanocatalysts with High Performance in Oxygen Electrode Reactions

Tao Zhang, Shuai-Chen Li, Wei Zhu, Zhi-Ping Zhang, Jun Gu and Ya-Wen Zhang*

Beijing National Laboratory for Molecular Sciences, State Key Laboratory of Rare Earth Materials Chemistry and Applications, PKU-HKU Joint Laboratory in Rare Earth Materials and Bioinorganic Chemistry, College of Chemistry and Molecular Engineering, Peking University, Beijing 100871, China. Fax: +86-10-62756787; E-mail: ywzhang@pku.edu.cn.

Table S1. Surface atomic ratios, proportions of oxidation states and OER mass activities of Pt-Ir NOs with different annealing temperatures.

Sample	Pt (%)	Ir (%)	Pt^{n+}/Pt (%)	Ir^{n+}/Ir (%)	Mass activity ($A\ g^{-1}$)
NO-300	68.3	31.7	44.1	68.2	15.7
NO-350	70.9	29.1	50.1	78.8	21.3
NO-400	69.4	30.6	67.9	100.0	27.9

Table S2. Surface atomic ratios of Pt-Ir alloy nanocrystals after annealing or working potential treatment determined from XPS analysis.

Sample	Annealed		Treated	
(%)	Pt	Ir	Pt	Ir
NO	74.5	25.5	70.9	29.1
NTO	70.4	29.6	68.7	31.3
NC	76.3	23.7	83.1	16.9
NSC	65.6	34.4	62.4	37.6
NW	74.1	25.9	70.8	29.2

Table S3. Electrochemically active surface area (ECSA) from the Cu-UPD and high frequency impedance of the catalysts.

Sample	ECSA ($m^2\ g^{-1}$)	R (Ω)	Sample	ECSA ($m^2\ g^{-1}$)	R (Ω)
NO	25.5	4.0	NW	7.5	4.1
NTO	20.4	4.0	Ir/C	23.3	4.1
NC	25.7	4.0	Pt/C	64.8	3.7
NSC	11.6	4.1	Pt/C-Ir/C	48.9	4.0

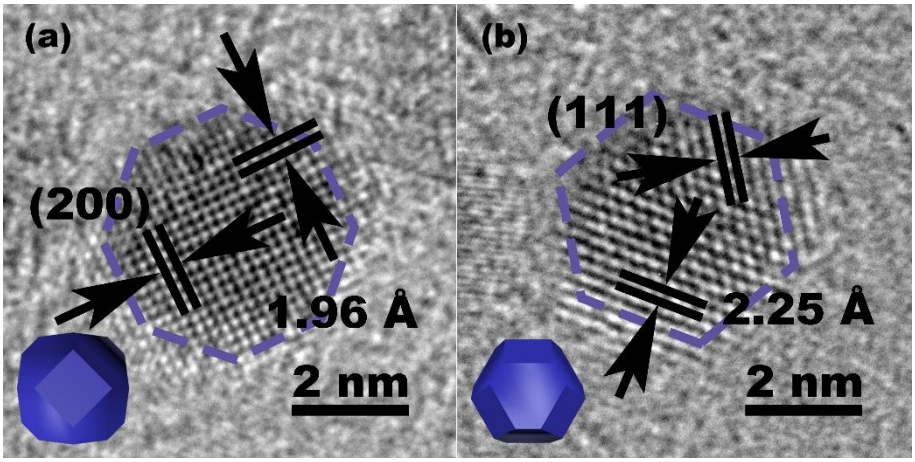

Fig. S1. HRTEM images of Pt-Ir alloy NTOs from the (a) (100) and (b) (111) facets view.

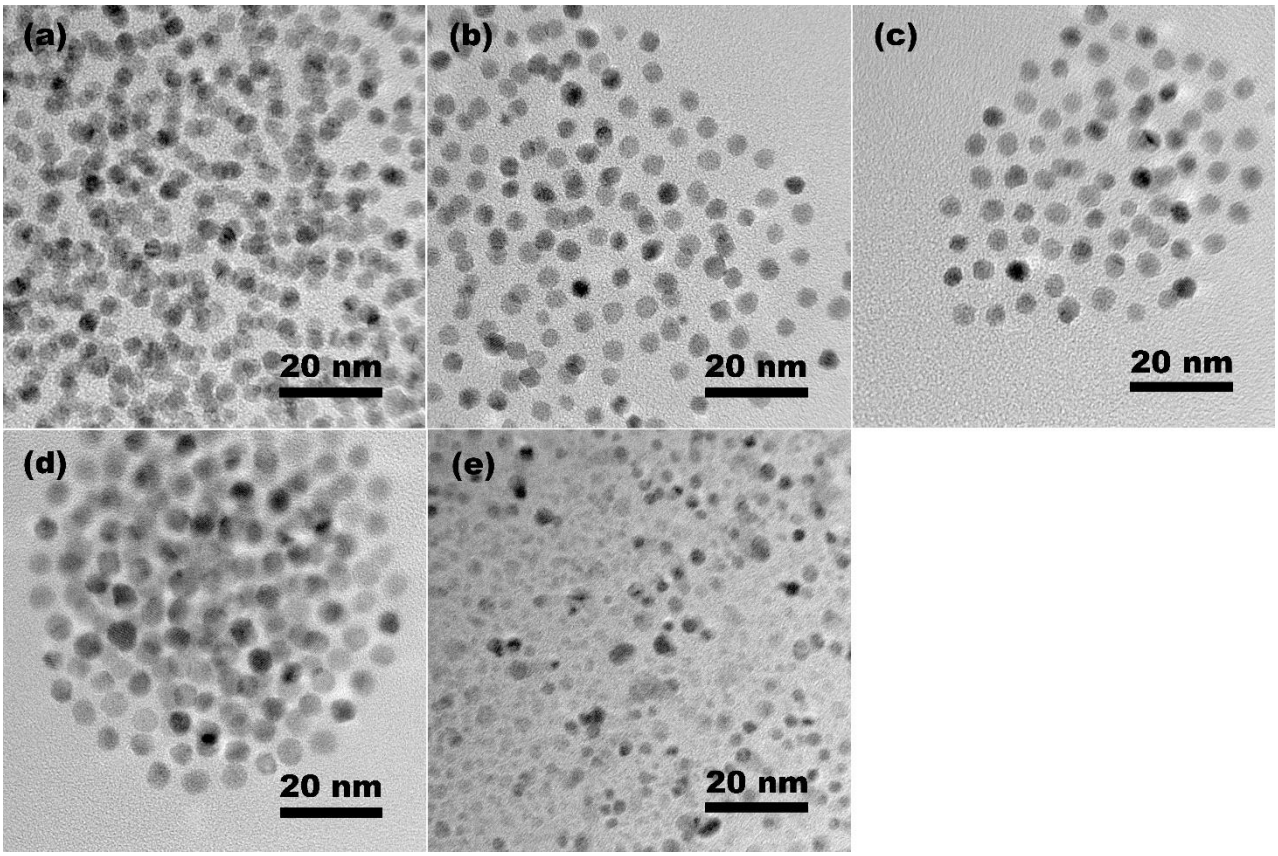

Fig. S2. TEM images of Pt-Ir nanoparticles obtained with different amounts of KBr: (a) without KBr, (b) 70 mg, (c) 700 mg, (d) 1400 mg. (e) TEM images of Pt-Ir nanoparticles obtained with 99 mg of TEAC. All the other conditions were the same as those of Pt-Ir alloy single-crystalline nanocrystals.

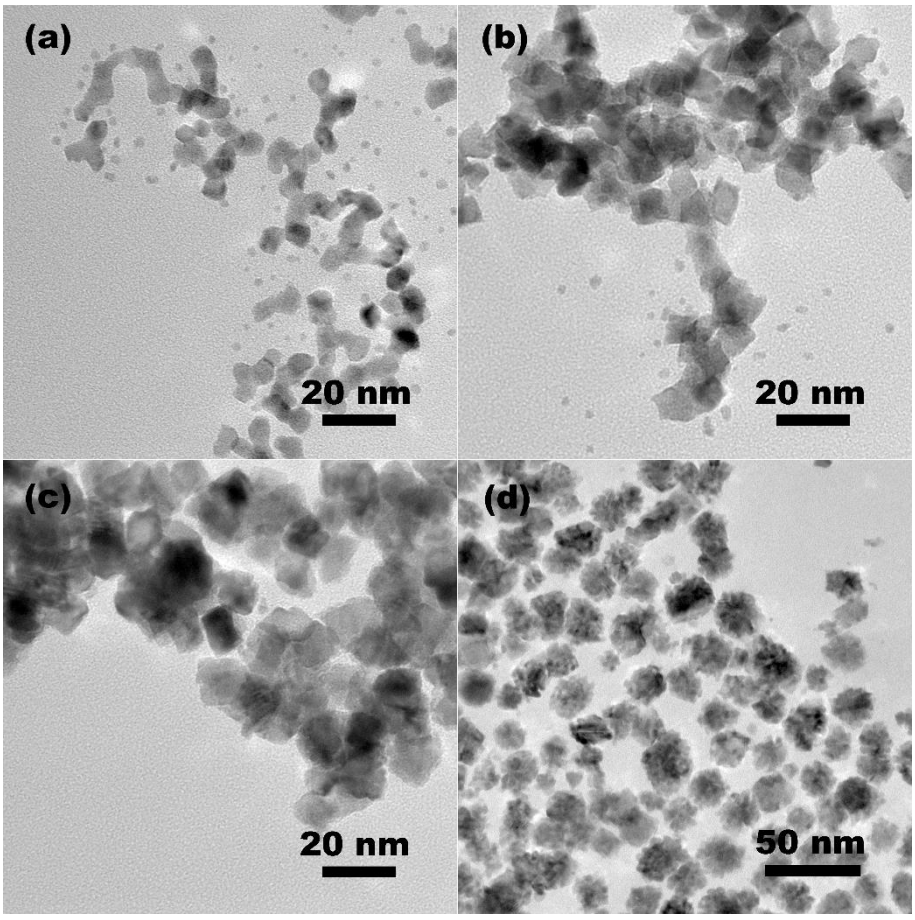

Fig. S3. TEM images of Pt-Ir nanoparticles obtained under different reaction conditions: (a) with 4 mg KI (b) with 20 mg KI (c) with 100 mg KI (d) with 500 mg KI. All the other conditions were the same as those of Pt-Ir alloy single-crystalline nanocrystals.

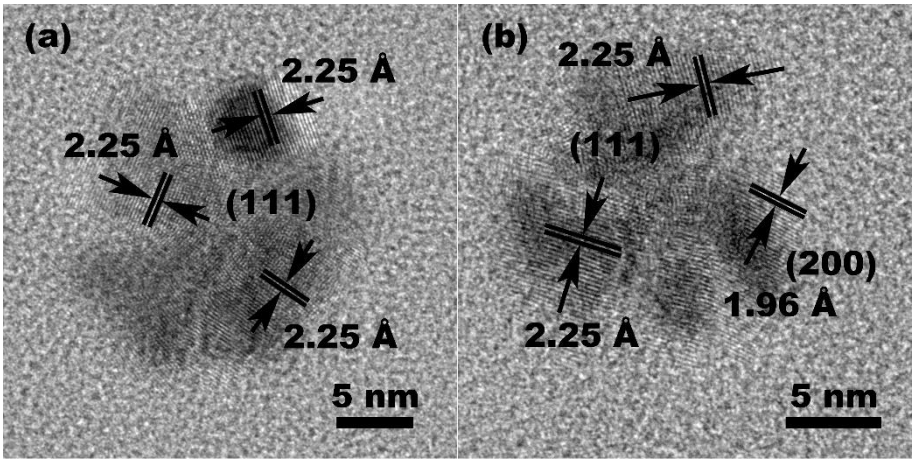

Fig. S4. HRTEM images of as-synthesized Pt-Ir NCFs.

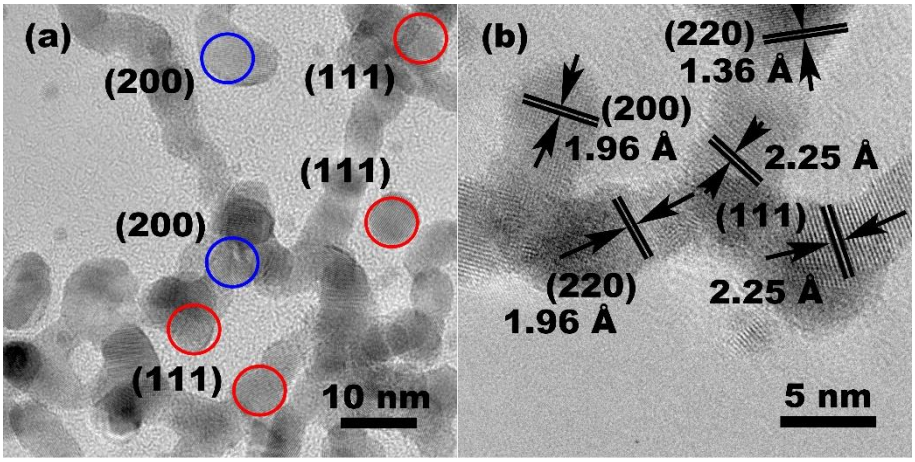

Fig. S5. HRTEM images of as-synthesized Pt-Ir worm-like NWs.

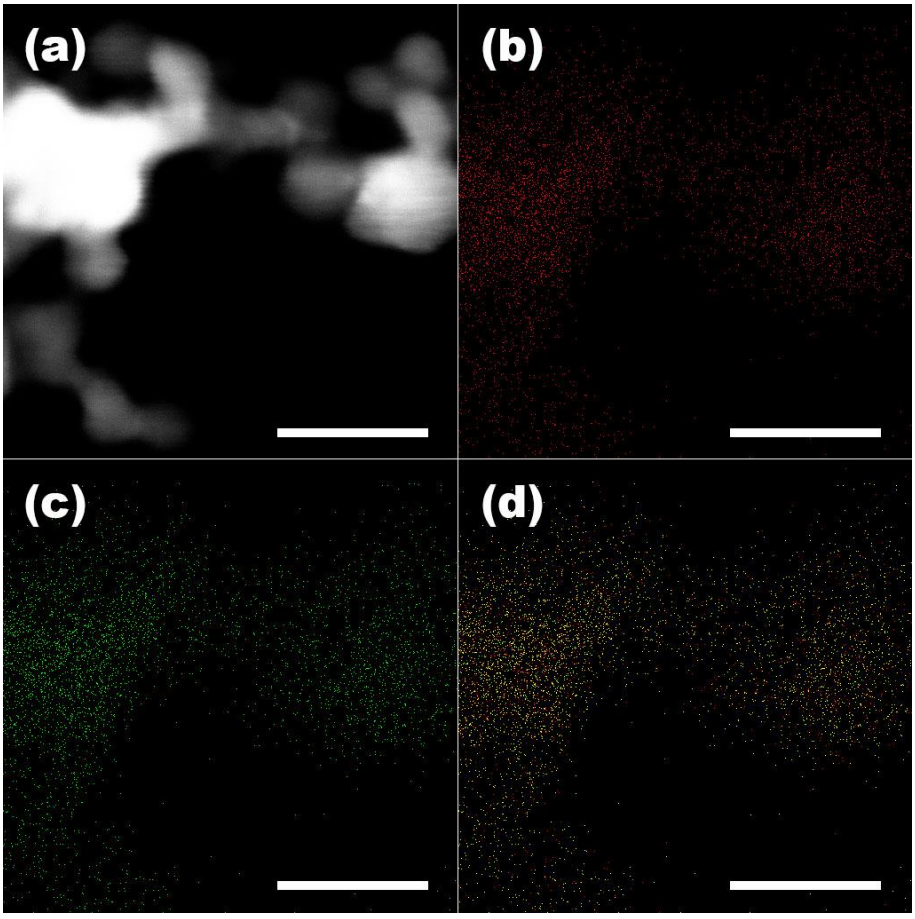

Fig. S6. HAADF-STEM image (a) and EDS mapping images: (b) Pt, (c) Ir, (d) overlay of as-synthesized Pt-Ir worm-like NWs with the scale bar of 20 nm.

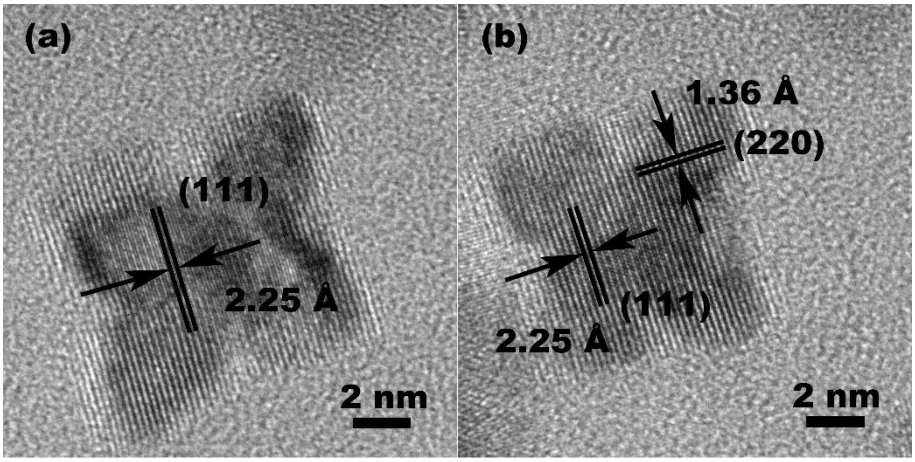

Fig. S7. HRTEM images of as-synthesized Pt-Ir NOSs.

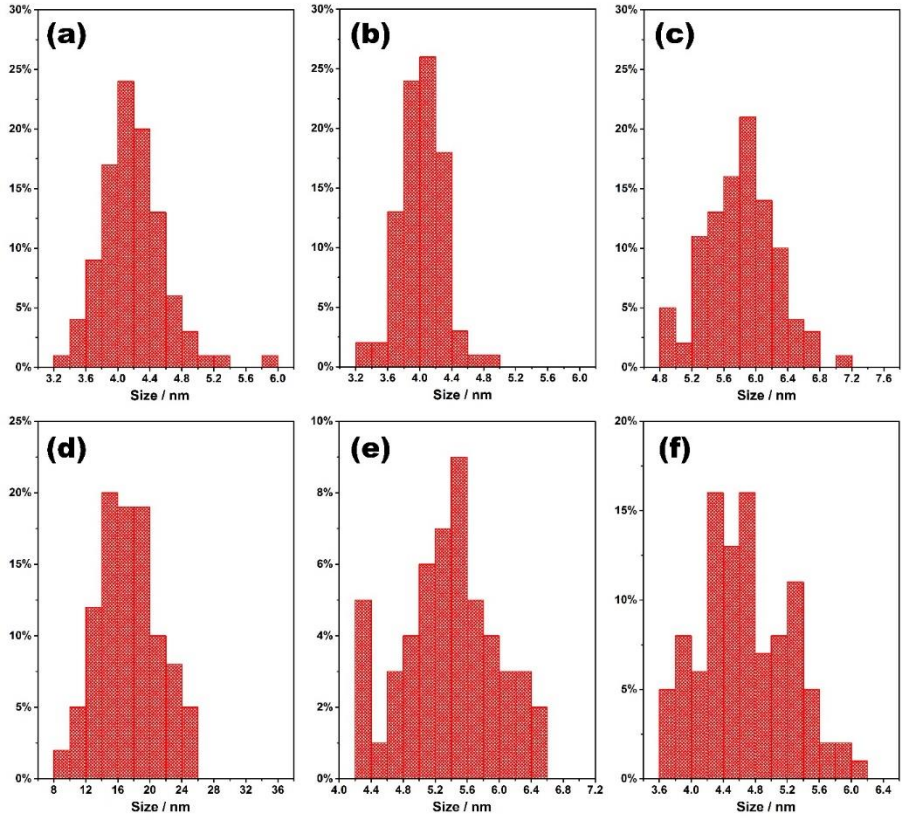

Fig. S8. Particle size statistics for as-synthesized Pt-Ir alloy nanocrystals: (a) NOs, (b) NTOs, (c) NCs, (d) NCFs, (e) NWs, and (f) NOSs.

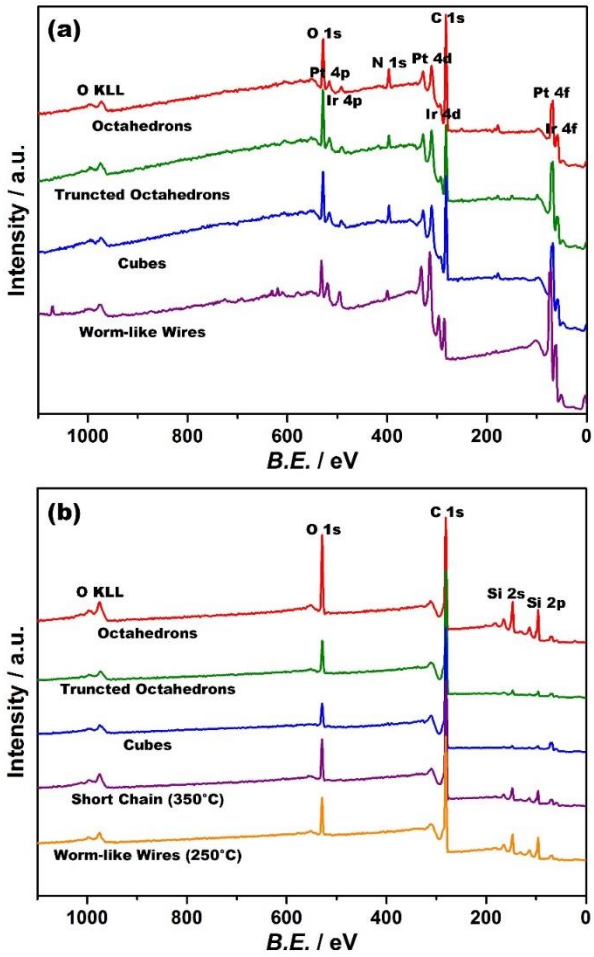

Fig. S9. XPS full spectra of Pt-Ir alloy nanocrystals (a) before and (b) after the annealing treatment.

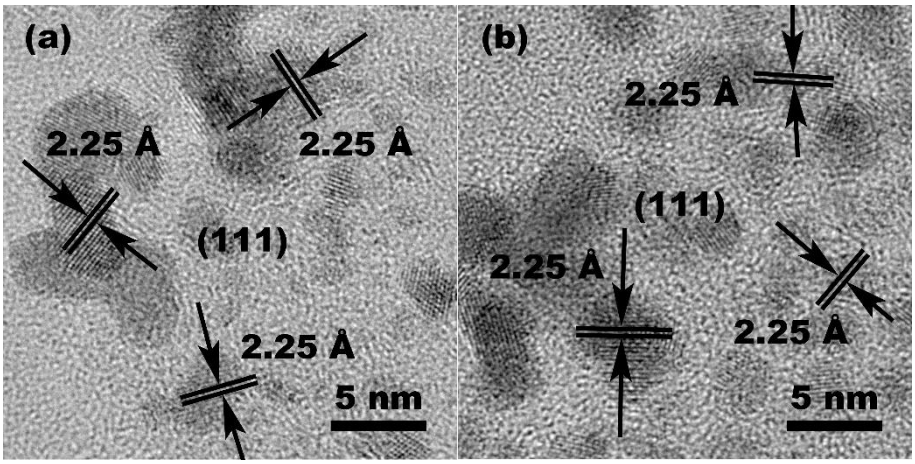

Fig. S10. HRTEM images of commercial Pt/C catalyst.

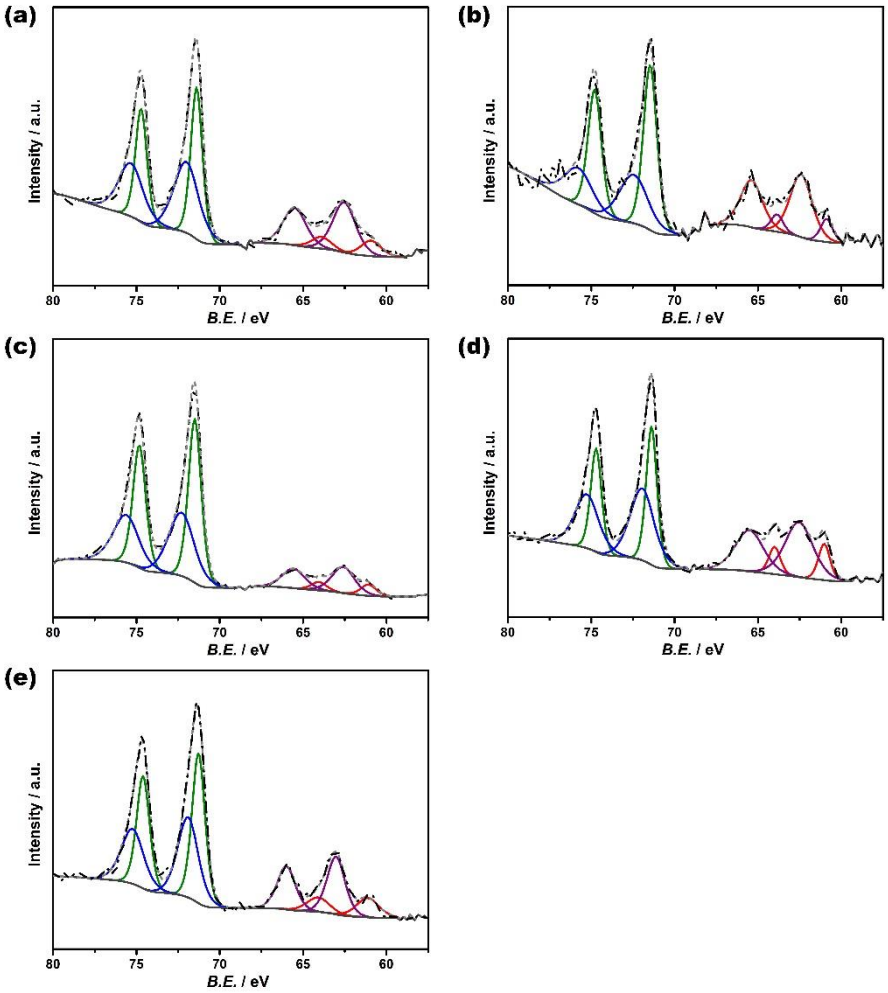

Fig. S11. XPS spectra of Pt-Ir alloy nanocrystals in Pt and Ir 4f regions after a working potential treatment at 1.479 V: (a) NOs, (b) NTOs, (c) NCs, (d) NSCs, and (e) NWs.

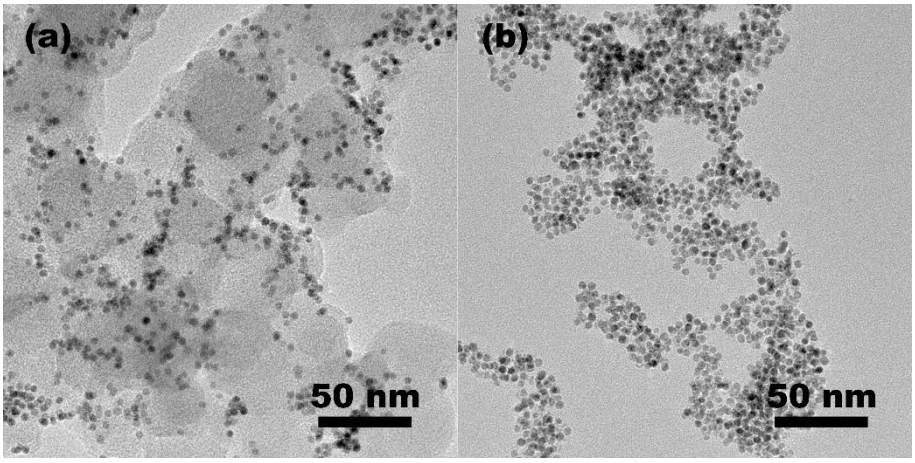

Fig. S12. TEM images for Pt-Ir NOs catalyst with different annealing temperatures: (a) NO-300, (b) NO-400.

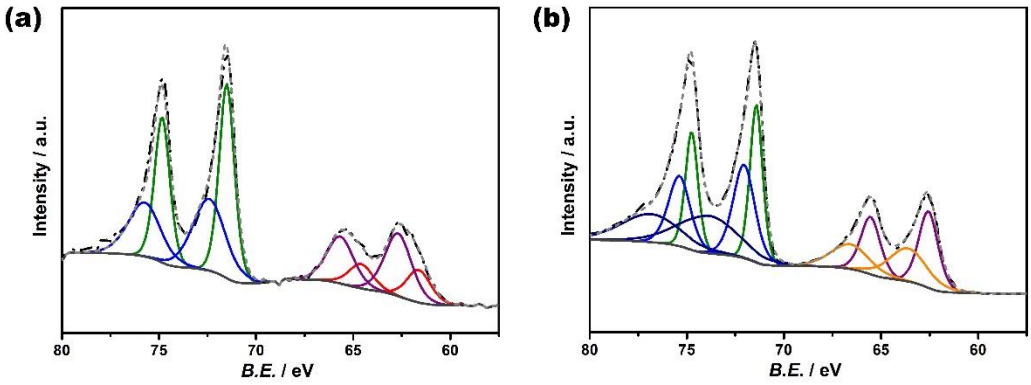

Fig. S13. XPS spectra of Pt-Ir NOs in Pt and Ir 4f regions after a working potential treatment at 1.479 V: (a) NO-300, (b) NO-400.

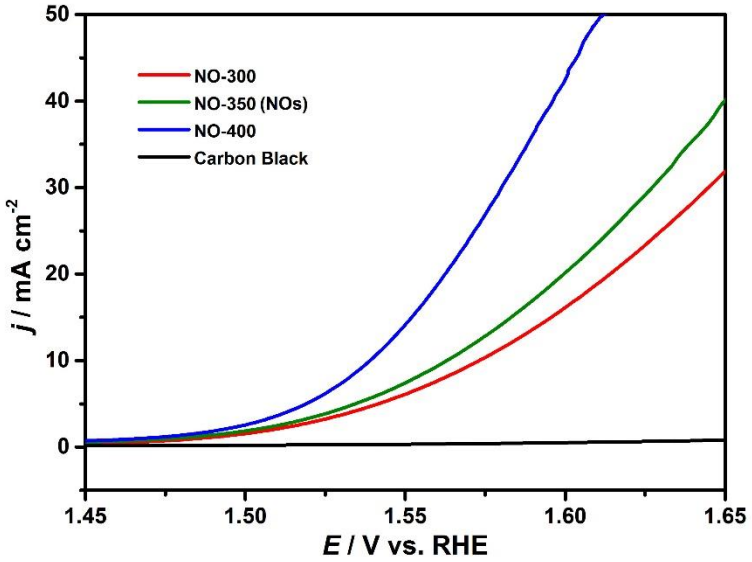

Fig. S14. IR-compensated polarization curves of carbon black and Pt-Ir NOs with different annealing temperatures in a N_2-saturated 0.5 mol L^{-1} H_2SO_4 electrolyte with a rotation rate of 1600 rpm at a sweep rate of 10 mV s^{-1}.

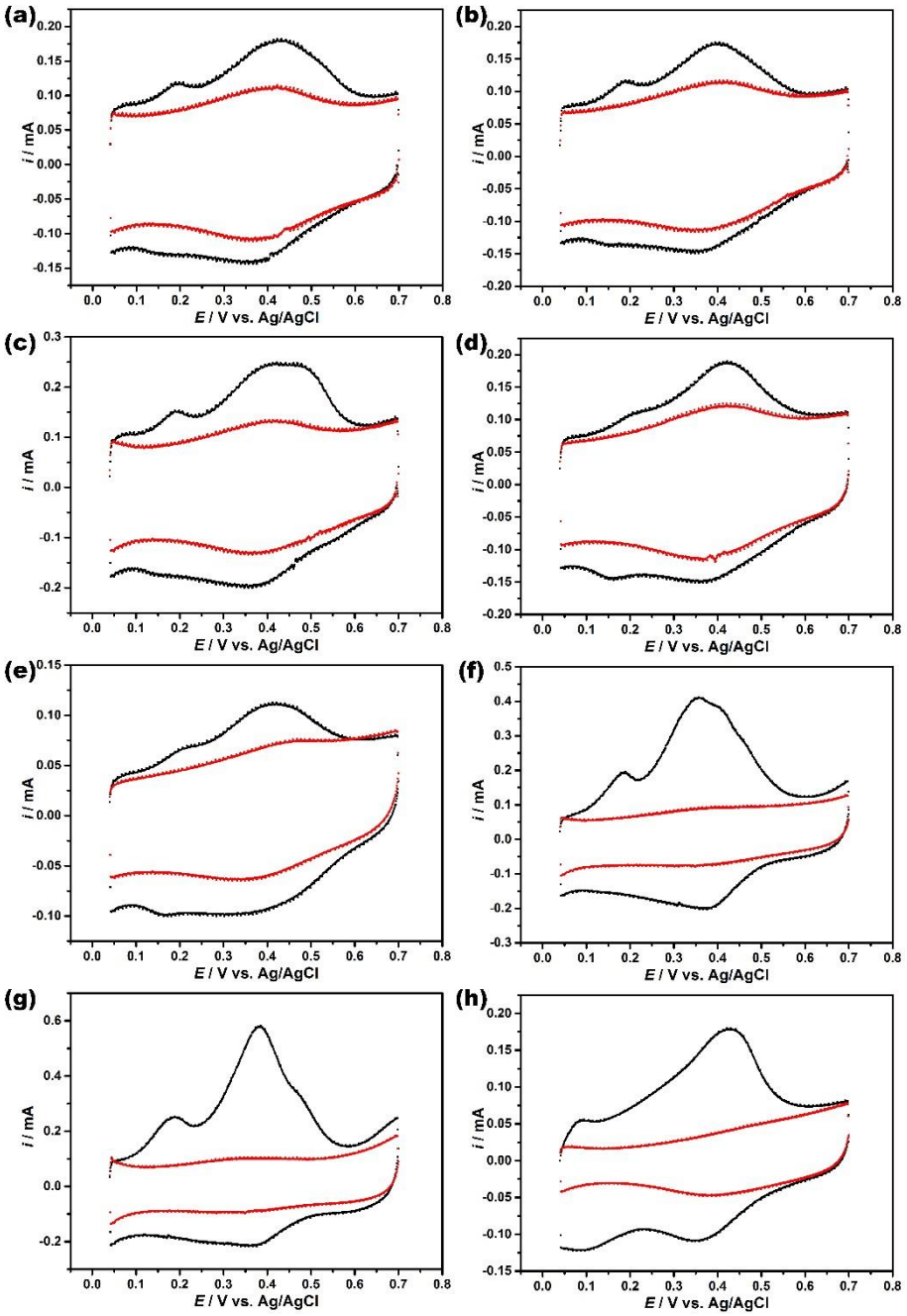

Fig. S15. Cu-UPD stripping curves measured at 0.3 V for 100 s in 2 mmol Ł$^{-1}$ $CuSO_4$ and 0.5 mol Ł$^{-1}$ H_2SO_4 solution (black curves) or 0.5 mol Ł$^{-1}$ H_2SO_4 solution (red curves), followed by the collection of CV curves from 0.04 V to 0.7 V vs. Ag/AgCl with the sweep rate of 50 mV s^{-1}: (a) NOs, (b) NTOs, (c) NCs, (d) NSCs, (e) NWs, (f) Pt/C-Ir/C mixture, (g) commercial Pt/C catalyst, and (h) commercial Ir/C catalyst. The ECSA of the sample was calculated from the stripping charge with the coefficient of 420 μC·cm^{-2}.

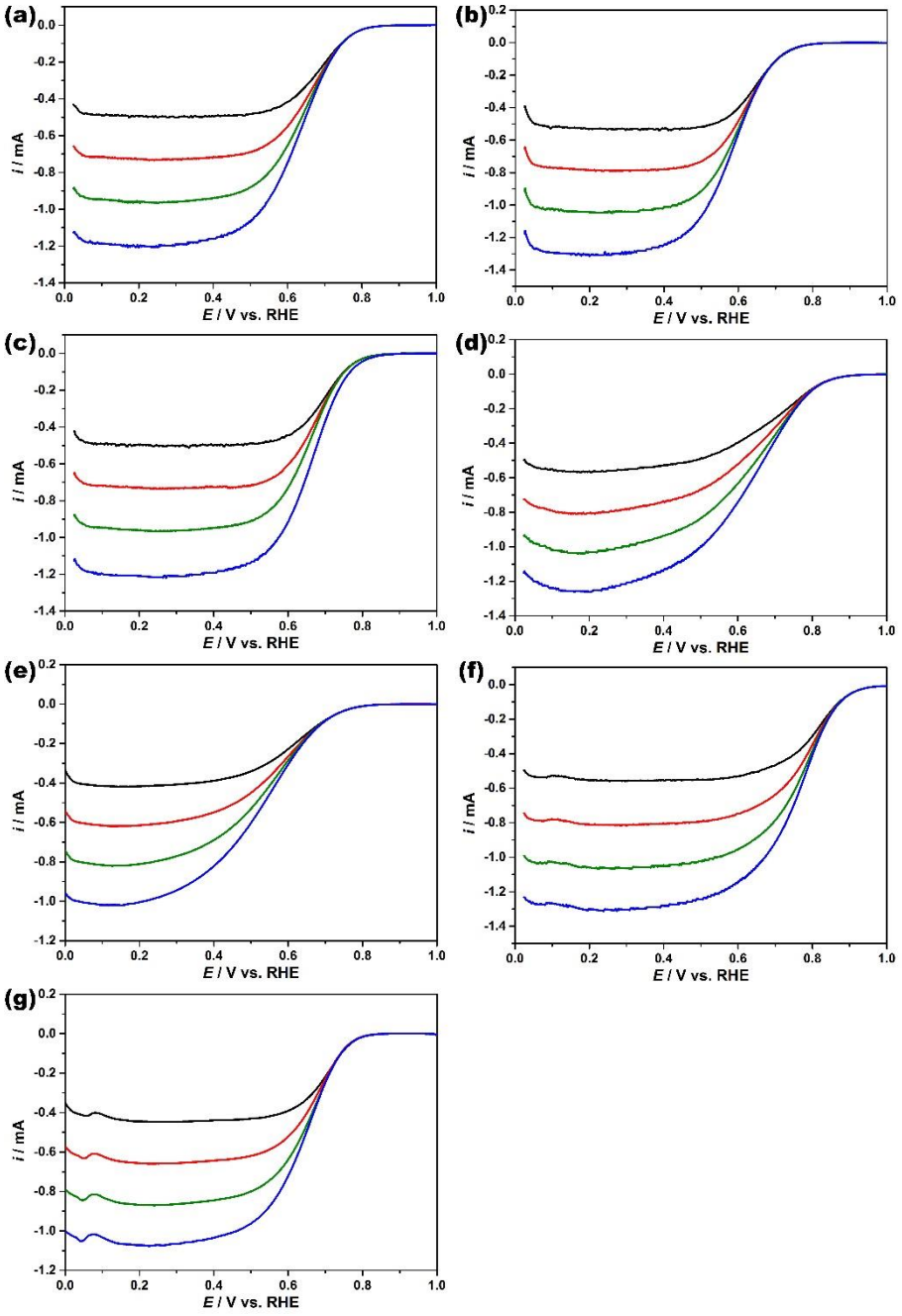

Fig. S16. Polarization curves for ORR on carbon black supported Pt-Ir alloy nanocatalysts and commercial Pt/C catalyst with different rotations (black: 400 rpm; red: 900 rpm; green: 1600 rpm; blue: 2500 rpm): (a) NOs, (b) NTOs, (c) NCs, (d) NSCs, (e) NWs, (f) commercial Pt/C catalyst, and (g) Pt/C-Ir/C mixture.

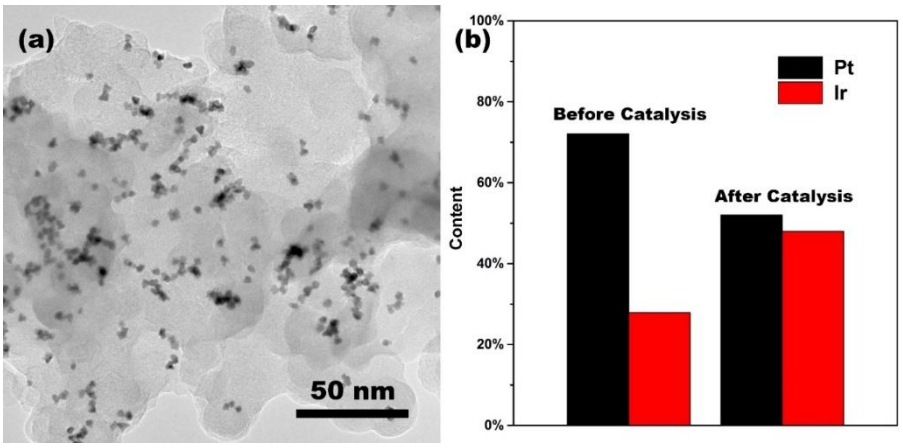

Fig. S17. TEM image (a) of Pt-Ir NSCs after 5000 cycles of voltage sweeps in the range of 0.6-1.0 V vs. RHE with a scan speed of 200 mV s^{-1} in O_2-saturated mol L^{-1} H_2SO_4 electrolyte. (b) Comparison of atomic content of Pt-Ir NSCs (from EDS) before and after the voltage sweeps.